THE APPLICATION OF PSO TO JOINT INVERSION OF MICROTREMOR RAYLEIGH WAVES DISPERSION CURVES AND REFRACTION TRAVELTIMES

R. POORMIRZAEE[1], R. HAMIDZADEH MOGHADAM[1] and A. ZAREAN[2]

[1] *Faculty of Mining Engineering, Sahand University of Technology, Tabriz, Iran.*
rashed.poormirzaee@gmail.com
[2] *Department of Civil Engineering, Shabestar Branch, Islamic Azad University, Shabestar, Iran.*
a.zarean@iaushab.ac.ir

(Received February 1, 2015; revised version accepted May 25, 2015)

ABSTRACT

Poormirzaee, R., Hamidzadeh Moghadam, R. and Zarean, A., 2015. The application of PSO to joint inversion of microtremor Rayleigh waves dispersion curves and refraction traveltimes. *Journal of Seismic Exploration*, 24: 305-325.

The accurate estimation of shear wave velocity (V_S) by Rayleigh wave dispersion analyses is very important for geotechnical and earthquake engineering studies, but dispersion curve inversion is challenging for most inversion methods due to its high nonlinearity and mix-determined trait. In order to overcome these problems, the current study proposes a joint inversion scheme based on a particle swarm optimization (PSO) algorithm. Seismic data considered for designing the objects were the Rayleigh wave dispersion curve and seismic refraction traveltime. For joint inversion, the objective functions were combined into a single function. The proposed algorithm was tested on two synthetic datasets and also on an experimental dataset. Synthetic models demonstrated that the joint inversion of Rayleigh wave and traveltime returned a more accurate estimation of V_S compared with single inversion Rayleigh wave dispersion curves. To verify the applicability of the proposed method, it was applied at a sample site in Tabriz city, northwestern Iran. For a real dataset, the refraction microtremor (ReMi) was used as a passive method for obtaining Rayleigh wave dispersion curves. Using PSO joint inversion, a three-layer subsurface model was delineated: the first layer's velocity was 316 m/s and its thickness was 5.5 m, the second layer's velocity was 280 m/s and its thickness was 2.8 m, and the last layer's velocity was 512 m/s. The results of synthetic datasets and the field dataset showed that the proposed joint inversion technique significantly reduces the uncertainties of inverted models and improves the revelation of boundaries.

KEY WORDS: joint inversion, Rayleigh wave, dispersion curves, traveltime, PSO, refraction microtremor.

0963-0651/15/$5.00

INTRODUCTION

Seismic surveying techniques provide data relevant to soil behavior at a very low strain level for large portions of soil tested in an undisturbed state by using procedures that are time- and cost-effective (Foti et al., 2003). Shallow shear-wave velocity (V_S) has long been recognized as a key factor in variable ground-motion amplification and site response in sedimentary basins (Stephenson et al., 2005). Velocity profiles together with the depth of the basement below the sediments are useful data in geotechnical studies for the correct construction of buildings (García et al., 2014). V_S structure is important for site effect studies and geotechnical engineering, but it is quite difficult and expensive to derive from conventional geophysical techniques (Mahajan et al., 2012). Current techniques for estimating shallow shear wave velocities to assess earthquake site response are too costly for use at most construction sites. They require large sources to be effective in noisy urban settings or specialized independent recorders laid out in an extensive array (Louie, 2001).

The Refraction Microtremor (ReMi) method (Louie, 2001) is a passive-source, multi-channel method that uses a linear array configuration. The ReMi method provides an effective and efficient means to obtain general information about large volumes of the subsurface in one dimension per setup, where appropriate setup length is related to the desired depth of investigation (Rucker, 2003). ReMi is based on obtaining the dispersion curve of the Rayleigh waves, but in this case, using ambient seismic noise or microtremors. For the processing procedure as in other surface wave methods, first, dispersion curves are constructed. The next step is to invert the dispersion curve to obtain a single V_S profile. The inversion stage in the processing of ReMi data, because of the data's nonlinearity and multi-dimensionality, is an important factor in achieving a reliable V_S profile.

Surface wave inversion is strongly non-linear, ill-posed, and mix-determined, and this leads to strong solution non-uniqueness as evidenced by several authors (Foti et al., 2003). In order to overcome these problems, constrain the interpretation, and decrease the uncertainty in estimating structures, a joint inversion scheme based on the PSO algorithm is proposed. Inverting the recorded datasets separately may lead to the incorrect interpretation for an underground structure; i.e., for an underground model with a high velocity layer overlying a low velocity layer, neither seismic refraction nor seismic reflection alone is able to resolve the parameters of the low velocity layer (Herring et al., 1995). The information for water table and bedrock and layer interface can be obtained by seismic refraction. Whereas dispersion curves do not give any information about the number of layers, refraction traveltimes, in principle, could (Dal Moro, 2008). Therefore, it is possible to reduce the intrinsic weakness of each method by integrating surface waves and refraction traveltime.

For joint inversion by PSO algorithm, the global criterion method, in which all misfit functions (i.e., objective functions) are combined to form a single function, was used. By finding the global minimum of misfit function, the best solution for the problem was obtained. The PSO algorithm is a global optimization method that belongs to the group of metaheuristic searching algorithms. In geophysical surveys, several significant PSO applications have recently emerged. Fernández Martínez et al. (2010a) presented the application of a whole family of PSO algorithms to analyze and solve a VES inverse problem associated with seawater intrusion in a coastal aquifer in southern Spain. Pekşen et al. (2011) inverted self-potential (SP) data by applying the PSO algorithm. Poormirzaee et al. (2014a) proposed a seismic traveltime inversion scheme based on the particle swarm optimization technique. Recently, Zarean et al. (2015) presented the application of mutation-based PSO algorithms to analyze the surface wave dispersion curves from microtremor records.

The proposed joint inversion algorithm was written and processed in MATLAB and tested on synthetic datasets. Finally, the reliability of the PSO joint inversion was investigated at a sample site in Tabriz, northwestern Iran to study site effects. The results for both synthetic and real datasets were compared with the single PSO inversion of ReMi data and also with a multi-objective optimization algorithm, the non-dominated sorting genetic algorithm-II (NSGA-II).

METHODOLOGY

Particle Swarm Optimization

PSO is a stochastic evolutionary computation technique for optimization in many different engineering fields which was inspired by the social behavior of individuals (called particles) in groups in nature, such as a flock (swarm) of birds searching for food (Kennedy and Eberhart, 1995). This algorithm searches the space of an objective function by adjusting the trajectories of individual agents, called particles, as these trajectories form piecewise paths in a quasi-stochastic manner (Yang, 2010). The particles move toward promising regions of the search space by exploiting information springing from their own experience during the search as well as the experience of other particles. For this purpose, a separate memory is used where each particle stores the best position (x_i^*) it has ever visited in the search space. The best position of each particle experience comprises other ones, and then the best position, which belongs to a minimum of misfit function, is selected as the global best (g^*). This procedure (i.e., finding x_i^*, g^*) is repeated for a certain iteration. Finally, the best global g^* is determined as the optimum solution. The movement of particles is schematically represented in Fig. 1.

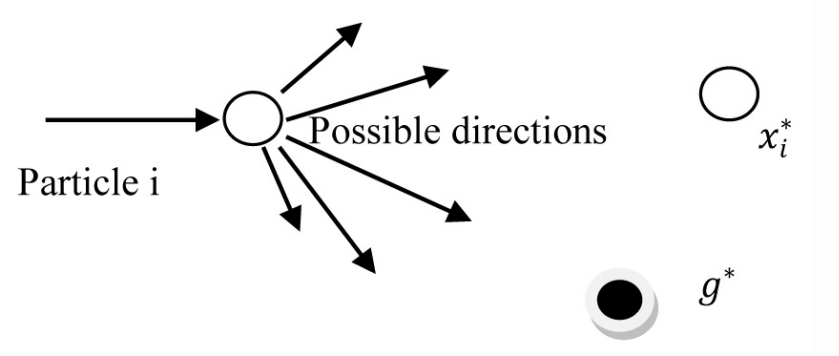

Fig. 1. Schematic representation of the motion of a particle in PSO, moving towards the global best g* and the current best x_i^* for each particle i (Yang, 2010).

Particle swarm consists of a swarm of particles, each moving or flying through the search space according to velocity update eq. (1) (Kennedy and Eberhart, 1995). The velocity of each particle is modified iteratively by its personal best position, and the best position found by particles in its neighborhood. v_i is the velocity of the i-th particle in the swarm, x_i is the particle position, x_i^* denotes the personal best position, and g* is the best position found by particles in its neighborhood.

$$v_i^{t+1} = v_i^t + \alpha\epsilon_1 \odot (g^* - x_i^t) + \beta\epsilon_2 \odot (x_i^* - x_i^t) \quad . \tag{1}$$

In eq. (1), ϵ_1 and ϵ_2 are two random vectors, and each entry takes a value between 0 and 1. The Hadamard product of two matrices $u \odot v$ is defined as the entry-wise product. The parameters α and β are the learning parameters or acceleration constants, which can typically be taken as, say, $\alpha \approx \beta \approx 2$ (Yang, 2010).

The initial locations of all particles should distribute relatively uniformly so that they can sample over most regions, which is especially important for multimodal problems. The initial velocity of a particle can be taken as 0, that is, $v_i^{t=0} = 0$. The new position can then be updated by eq. (2) (Yang, 2010),

$$x_i^{t+1} = x_i^t + v_i^{t+1} \quad . \tag{2}$$

A number of variations on the original PSO have been proposed to overcome its shortcomings and drawbacks, such as slow convergence and wandering near the global minimum in the final search stage. One of the most notable of these formulations is the introduction of an inertia weight by Shi and Eberhart (1998). An inertia term (i.e., static inertia weight) $\omega \in (0,1)$ is introduced into the original PSO velocity rule as follows:

$$v_i^{t+1} = \omega v_i^t + \alpha\epsilon_1 \odot (g^* - x_i^t) + \beta\epsilon_2 \odot (x_i^* - x_i^t) \quad . \tag{3}$$

As long as $\omega \in (0,1)$, the velocity update, eq. (3), helps particles forget their lower-quality past positions in order to be more affected by the higher-quality information of late, which seems to make more sense conceptually (Evers, 2009).

For ω, α and β, there are several popular parameter sets in the literature (Table 1). Another notable recent variation on the original PSO algorithm is the introduction of the so-called constriction factor by Clerc (1999). This method introduces a constriction factor $\chi \in (0,1)$ into the original velocity rule [eq.(1)], which effectively reduces the velocity of the particles as the search progresses, thereby contracting the overall swarm diameter. This in turn results in a progressively smaller domain being searched (Fernández Martínez et al., 2010b). Applying a constriction factor into PSO improves the convergence of the particles [eq. (4)]. Other parameters that are being used in different studies are listed in Table 1.

$$v_i^{t+1} = \chi[v_i^t + \alpha\epsilon_1 \odot (g^* - x_i^t) + \beta\epsilon_2 \odot (x_i^* - x_i^t)] \quad . \tag{4}$$

Table 1. Proposed PSO parameter sets in different references.

No. Set	PSO parameters				Reference
	α	β	χ	ω	
1	1.300	2.800	0.7298	-	Schutte and Groenwold (2005)
2	2.050	2.050	0.7290	-	Evers, (2009)
3	0.948	2.041	-	0.729	Carlisle and Dozier, (2001)
4	1.700	1.700	-	0.600	Trelea, (2003)
5	1.494	1.494	-	0.729	Clerc and Kennedy, (2002)
6	2.000	1.800	-	0.800	Fernández Martínez et al., (2010b)

ReMi and seismic refraction techniques

The ReMi technique is a cheaper and quicker "passive" geophysical technique. This method is based on ambient noise measurements that are carried out with seismic arrays to obtain information on surface wave velocity dispersion. Urban conditions, such as existing underground facilities and ambient noise due to cultural activity, restrict the general application of conventional geophysical techniques (Cha, 2006). The ReMi method combines the urban utility and ease of microtremor array techniques with the operational

simplicity of spectral analysis of the surface waves (SASW) technique and the shallow accuracy of the multi-channel analysis of surface waves (MASW) technique. As an SASW technique, ReMi is based on obtaining the dispersion curve of the Rayleigh waves, but in this case, using ambient seismic noise or microtremors. Configurations of 12 to 48 single vertical, 8-12 Hz exploration geophones can give surface-wave phase velocities at frequencies as low as 2 Hz and as high as 26 Hz. This range is appropriate for constraining shear velocity profiles from the surface to a depth of 100 m (Louie, 2001).

After Louie (2001), the reliability and accuracy of the ReMi method was investigated in different case studies. Rucker (2003) applied the ReMi shear wave technique for geotechnical characterization and discussed several geotechnical applications in his publication. Scott et al. (2004) performed a measurement of shear-wave velocity to a 30-m depth (V_{S30}) for a hazard assessment of the Reno basin. They were successful in obtaining a detailed shallow shear-wave velocity transect across an entire urban basin with minimum effort. Coccia et al. (2010) used the ReMi technique to determine the 1D shear wave velocity in a landslide area and concluded that in marginally stable slope areas, the ReMi method can provide the data needed to calculate shear wave velocity vertical profiles down to depths of few tens of meters. This can even be achieved by using an array shorter than the commonly recommended minimum value of 100 m. Panzera and Lombardo (2013) successfully used ReMi and MASW techniques to investigate the dynamic properties of main lithotypes outcropping in the Siracusa region and their relationships with the local seismic response. Poormirzaee and Hamidzadeh (2014) applied ReMi data in a study of V_S structure in an urban area where using other active seismic methods was limited.

The seismic refraction surveying method uses seismic energy that returns to the surface after traveling through the ground along refracted ray paths.The first arrival of seismic energy at a detector offset from a seismic source represents either a direct ray or a refracted ray (Kearey et al., 2002). On the local scale, refraction surveys are widely used in foundation studies at construction sites to derive estimates of depth to rockhead beneath a cover of superficial material. Refraction surveys find broad applications in exploration programs for underground water supplies in sedimentary sequences and are often employed in conjunction with electrical resistivity methods.

In general, the traveltime t_0 of a ray critically refracted along the top surface of the n-th layer is given by the following:

$$t_0 = (x/v_n) + \sum_{i=1}^{n-1} 2z_i \cos\theta_{in}/v_i \quad , \tag{5}$$

where $\theta_{in} = \sin^{-1}(v_i/v_n)$.

In eq. (5), x is the offset distance from shot point, v is the velocity of layer, z is the depth of refractor, and $\sin\theta = v_1/v_2$ is Snell's Law (Kearey et al., 2002).

Joint inversion of Rayleigh wave and refraction traveltime by PSO

The Rayleigh wave dispersion curves and refraction traveltimes are jointly inverted through a procedure based on PSO technique. The proposed algorithm's main goal is to improve the reconstruction of a subsurface structure by exploiting the complementary information attainable by Rayleigh wave dispersion and refraction traveltime. The Rayleigh wave dispersion inversion procedure was performed using the fundamental mode.

The most important parameters that influence Rayleigh wave propagation are shear wave velocity (V_S) and layer thickness, while density (ρ) and P-wave velocity (V_P) play minor roles (Xia et al., 1999). On the other hand, refraction traveltime depends on longitudinal velocity and thickness. In order to obtain accurate results in the joint inversion procedure, it was decided to link V_P and V_S by means of the Poisson ratio (σ). In this way, a generally wide range of Poisson values [0.1 - 0.48] is allowed for each layer. Of course, the suitable range of Poisson values is dependent upon the study area and can be determined through primary information. Using eq. (6) and the above-stated Poisson values, a straight equation is obtained [eq. (6)]. For each particle (i.e., the model), the V_P and V_S are checked to detect the V_P/V_S ratio. If this ratio exceeds the imposed limits, the algorithm for satisfying eq. (6) generates new random values for V_P and V_S.

$$V_P = V_S[\sqrt{(1-\sigma)} / \sqrt{(½-\sigma)}] \quad , \tag{6}$$

$$1.5 < V_P/V_S \; 5 \quad . \tag{7}$$

Moreover, the parameter of density was fixed according to the classical Gardner et al. (1974) empirical V_P-ρ relationship:

$$\rho = \log[0.23\ (kV_P)^{0.25}] \quad , \tag{8}$$

where K = 1/0.3048 is a constant to convert feet into meters.

For joint inversion of ReMi and seismic refraction data, the summation of the root mean square (RMS) error is considered the objective function (OBF). In order to solve the forward modeling and estimate the theoretical dispersion curve, the code based on the matrix algorithm developed by Herrmann (1987)

curve, the code based on the matrix algorithm developed by Herrmann (1987) was used. The root mean square misfit between the observed and calculated value of velocity is defined as the objective function (OBF_1) according to the following equation:

$$OBF_1 = \{[\sum_{j=1}^{n_p} (v^{obs} - v^{cal})^2]/n_p\}^{1/2} \quad , \tag{9}$$

where n_p is the number of samples, v^{obs} is the observed phase velocity, and v^{cal} is the calculated one.

Additionally, the forward algorithm used in the inversion is based on a 1D ray-tracing for the P-wave traveltimes. The root mean square misfit between the observed and calculated refraction traveltimes are defined as the object function (OBF_2) according to the following equation:

$$OBF_2 = \{[\sum_{j=1}^{n_p} (t^{obs} - t^{cal})^2]/n_p\}^{1/2} \quad , \tag{10}$$

where n_p is the number of points, t^{obs} is the observed traveltime, and t^{cal} is the calculated traveltime. For seismic refraction data, the forward algorithm used in the inversion is based on a 1D ray-tracing for the P-wave traveltimes.

In the joint inversion procedure, the elements of the objective function can have different physical dimensions and various orders of magnitude. Thus, to have stable results, normalization is needed (Herring et al., 1995). For normalization, the parameter values in the objective function are divided into its observed values (Eq. 11).

$$OBF = \left[\{[\sum_{j=1}^{n_p} (x^{obs} - x^{cal})]/x^{obs}\}^2/n_p\}\right]^{1/2} \quad , \tag{11}$$

where x^{obs} is the observed value and x^{cal} is the calculated value. The general flowchart of the PSO joint inversion algorithm is shown in Fig. 2. This algorithm was investigated in both synthetic and real datasets.

Synthetic dataset

To test the PSO joint inversion algorithm and evaluate its performance,

of the proposed joint inversion algorithm (PSO Joint Inv.), the obtained V_S profile was compared with the estimated V_S profile of the PSO single inversion of ReMi data (PSO Inv.) and also by the non-dominated sorting genetic algorithm (NSGA-II). In the PSO single inversion approach (Poormirzaee et al., 2014b), only ReMi data was inverted. The NSGA-II, proposed by Deb et al. (2000), is a modified version of the non-dominated sorting genetic algorithm (NSGA) proposed by Srinivas and Deb (1994). This algorithm as a multi-objective optimization algorithm has been investigated in many studies (Coello et al., 2004).

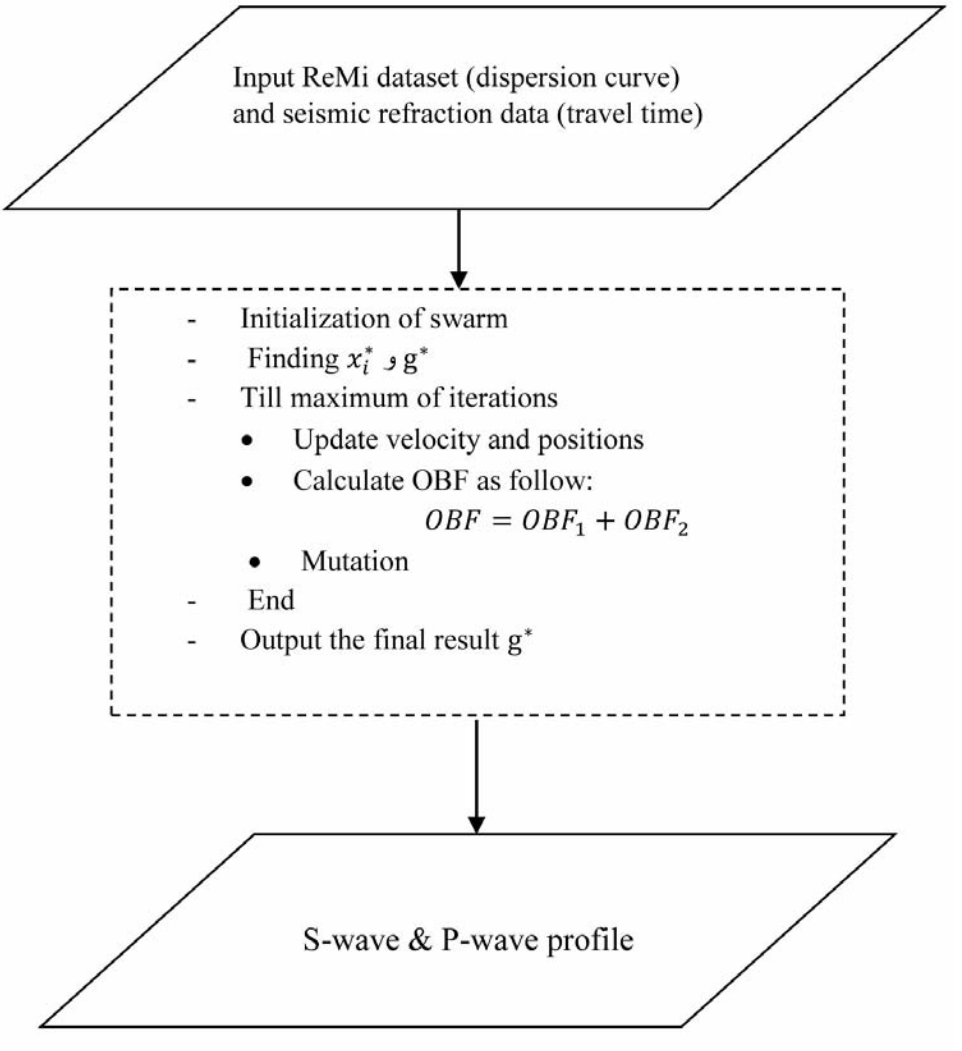

Fig. 2. PSO joint inversion algorithm to invert Rayleigh wave and traveltimes dataset.

Table 2. Parameters of the synthetic model A and search space.

Layer number	V_S(m/s)	V_P(m/s)	H(m)	Search space		
				V_P(m/s)	V_S(m/s)	H(m)
1	190	400	4	200-600	90-300	2-6
2	370	700	5	350-1050	150-550	2-7
3	220	430	5	200-600	100-300	2-7
4	700	1250	half space	700-2000	350-1000	-

To investigate the PSO joint inversion algorithm, first the 4-layer synthetic model reported in Table 2 (model A) was considered, and the particle and maximum numbers of iterations of 80 and 50, respectively, were selected. The adopted model was designed in order to reproduce a typical hidden-layer case which is clearly prone to erroneous refraction traveltime interpretation. The estimated dispersion curve and traveltime values are shown in Figs. 3a and 3b. The mean results obtained from different inversion algorithms for model A are shown in Table 3 and Fig. 3c.

Table 3. Mean model obtained from the model A by different inversion algorithm.

Parameters	PSO Inv. (ReMi data)	PSO joint Inv.	NSGA-II
V_S1(m/s)	192	197	227
V_S2(m/s)	442	358	283
V_S3(m/s)	208	251	212
V_S4(m/s)	670	720	560
H1(m)	4.4	4	4.05
H2(m)	4.3	4.8	5.2
H3(m)	5.5	5.3	5.4
V_P1(m/s)	472	386	401
V_P2(m/s)	668	664	705
V_P3(m/s)	500	522	350
V_P4(m/s)	1112	1119	965

Table 4. Parameters of the synthetic model B and search space.

Layer number	V_S(m/s)	V_P(m/s)	H(m)	Search space		
				V_P (m/s)	V_S(m/s)	H(m)
1	285	700	3	350-1050	142-427	1-5
2	163	400	2	200-600	80-244	1-3
3	600	1470	10	700-2100	300-900	5-15
4	1328	2300	half space	1150-3400	664-1900	-

The PSO joint inversion method was probed by a four layer model, model B. Table 4 shows model B and the search space used for inversion. The estimated dispersion curve and traveltime values are shown in Figs. 4a and 4b. The mean results obtained from inversion for model B is shown in Table 5 and Fig. 4c.

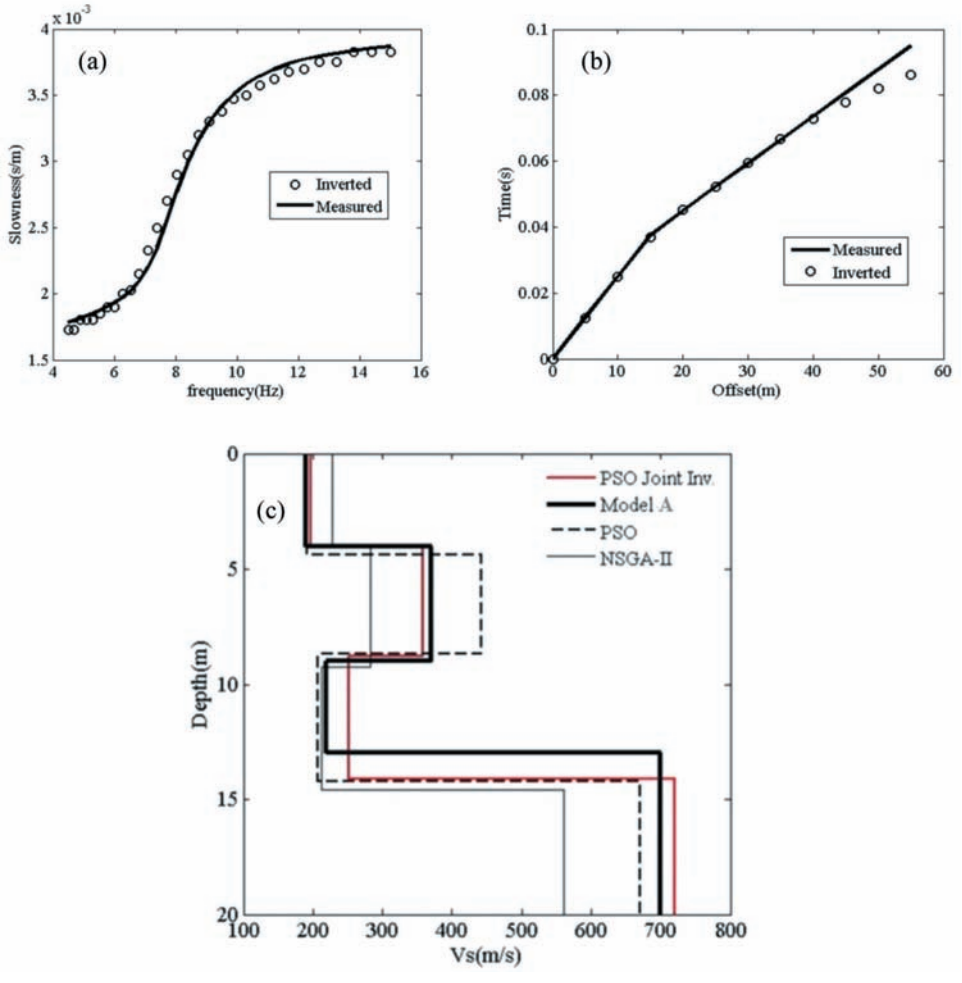

Fig. 3. a) Inversion of dispersion curve using PSO joint inversion for model A. b) Inversion of traveltimes using PSO joint inversion for model A. c) V_S profile of Model A, using PSO Joint Inv. (joint inversion of refraction and ReMi data), PSO (single inversion of ReMi data by PSO) and NSGA-II (joint inversion of refraction and ReMi data by NSGA-II).

Table 5. Mean model obtained from the model B.

Parameters	PSO Inv. (ReMi data)	PSO joint Inv.	NSGA-II
V_S1(m/s)	290	298	270
V_S2(m/s)	187	197	214
V_S3(m/s)	642	628	661
V_S4(m/s)	947	1326	1332
V_P1(m/s)	539	610	661
V_P2(m/s)	402	486	527
V_P3(m/s)	1420	1134	1611
V_P4(m/s)	2158	2195	1304
H1(m)	2.6	2.8	3
H2 (m)	2.4	1.8	3
H3 (m)	9.1	9.6	9.6

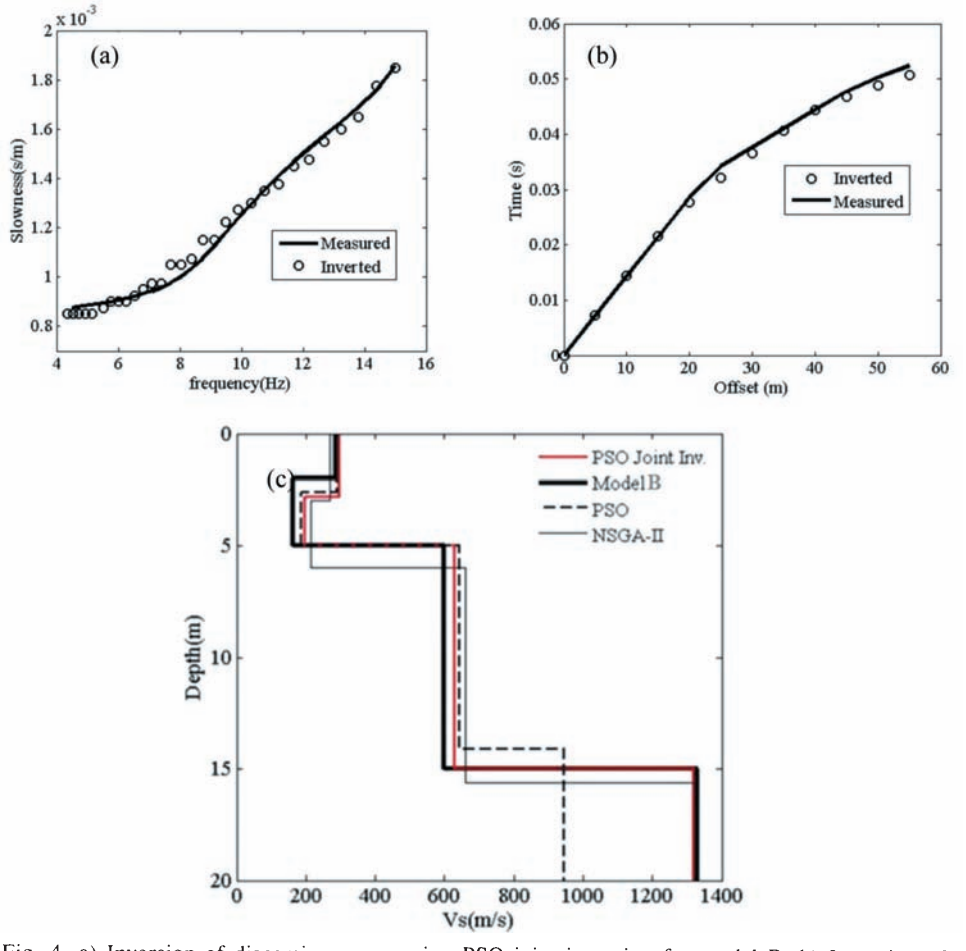

Fig. 4. a) Inversion of dispersion curve using PSO joint inversion for model B. b) Inversion of traveltimes using PSO joint inversion for model B. c) V_S profile of Model B, using PSO joint Inv.(joint inversion of refraction and ReMi data), PSO (single inversion of ReMi data by PSO) and NSGA-II (joint inversion of refraction and ReMi data by NSGA-II).

Field dataset

To further explore the applicability of the PSO joint inversion algorithm described above, ReMi and seismic refraction data was acquired in the city of Tabriz in northwestern Iran (Fig. 5). The datasets were reanalyzed in the present study using the PSO joint inversion approach. The data was collected in a profile line. In this study, the ReMi and seismic refraction method was performed using an OYO 24-channel seismograph and 4.5 Hz and 28 Hz geophones with a receiver spacing of 5 m. A total of 14 unfiltered 17-second records were collected at the study site. ReMi data processing consists of three steps: 1) preliminary detection of surface waves, 2) extraction of the dispersion curve, and 3) inversion of the dispersion curve. In this study, the module Pickwnin/SW of the commercial software package SeisImager v.3.1 was used to detect surface waves and obtain the dispersion curve (Fig. 6).

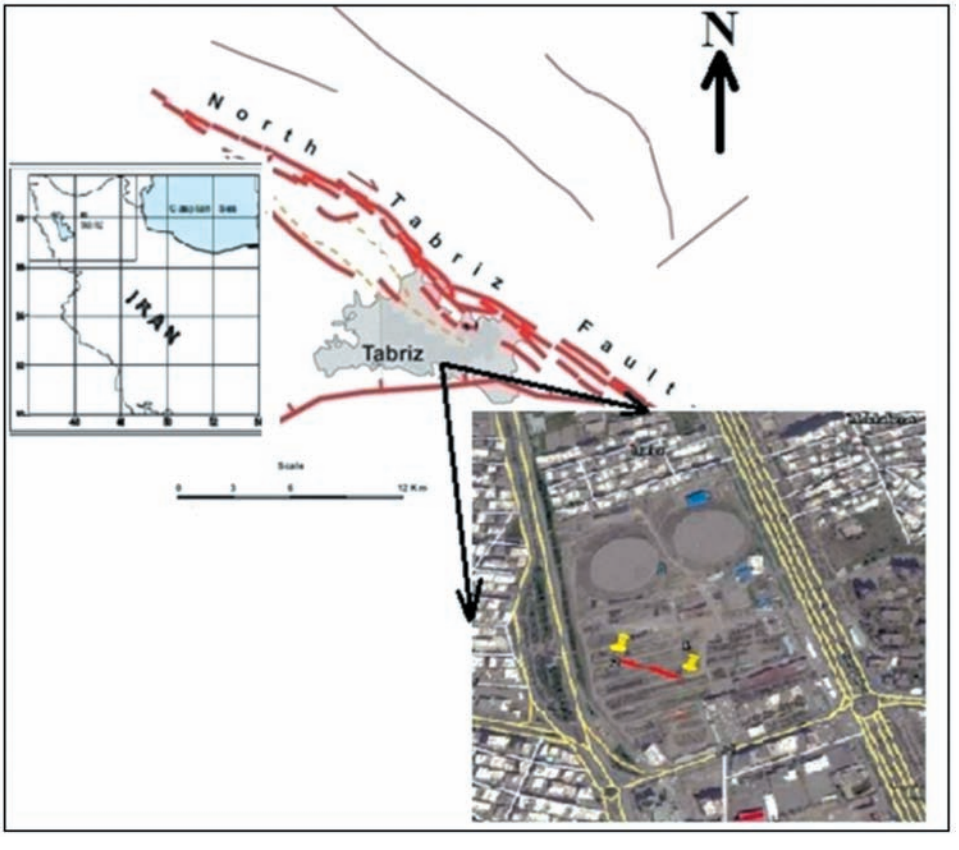

Fig. 5. Location of study area in Tabriz (NW of Iran).

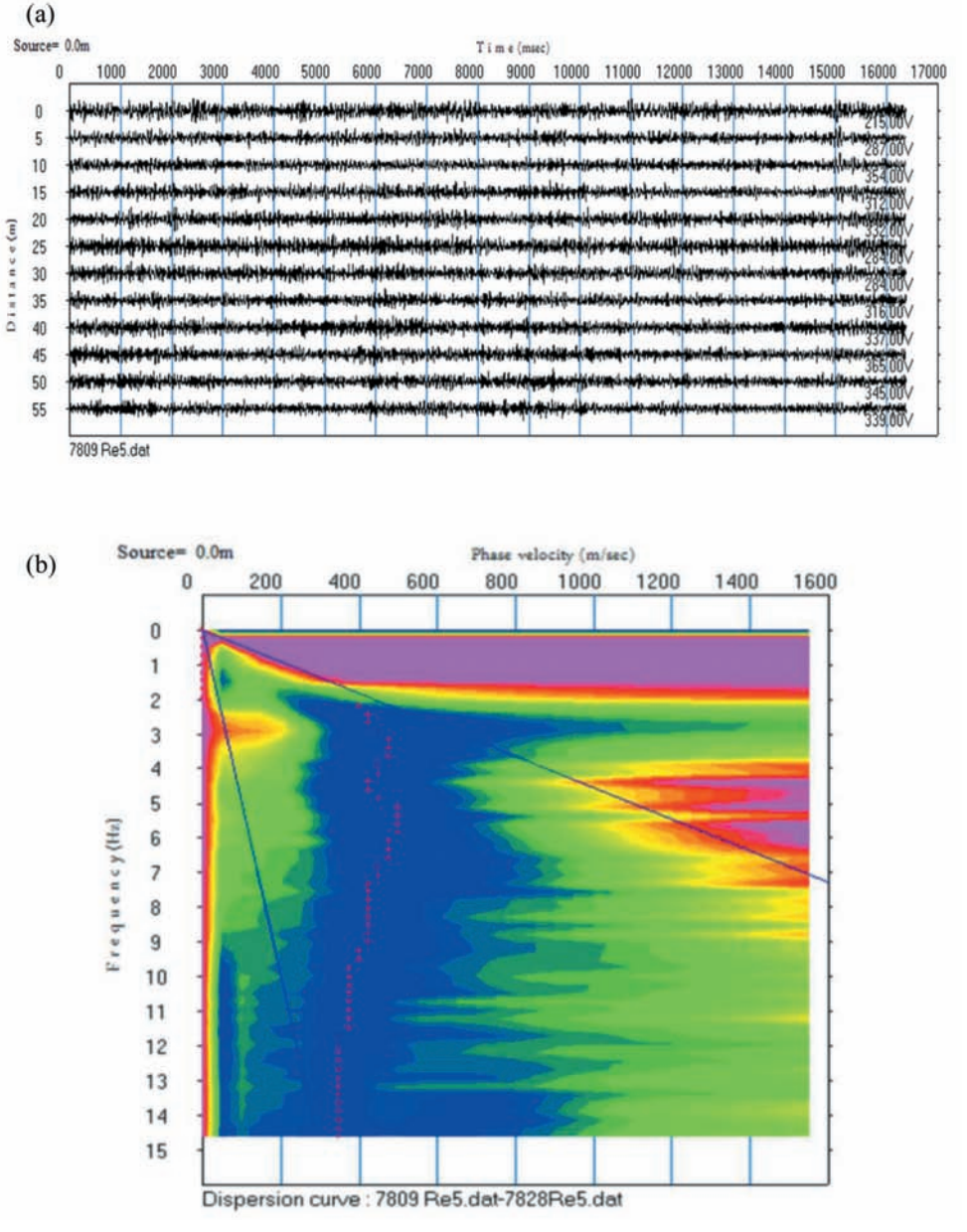

Fig. 6. Field dataset. a) A sample record of ReMi data, b) Dispersion curve (red points, the maximum amplitudes on the phase velocity-frequency plot).

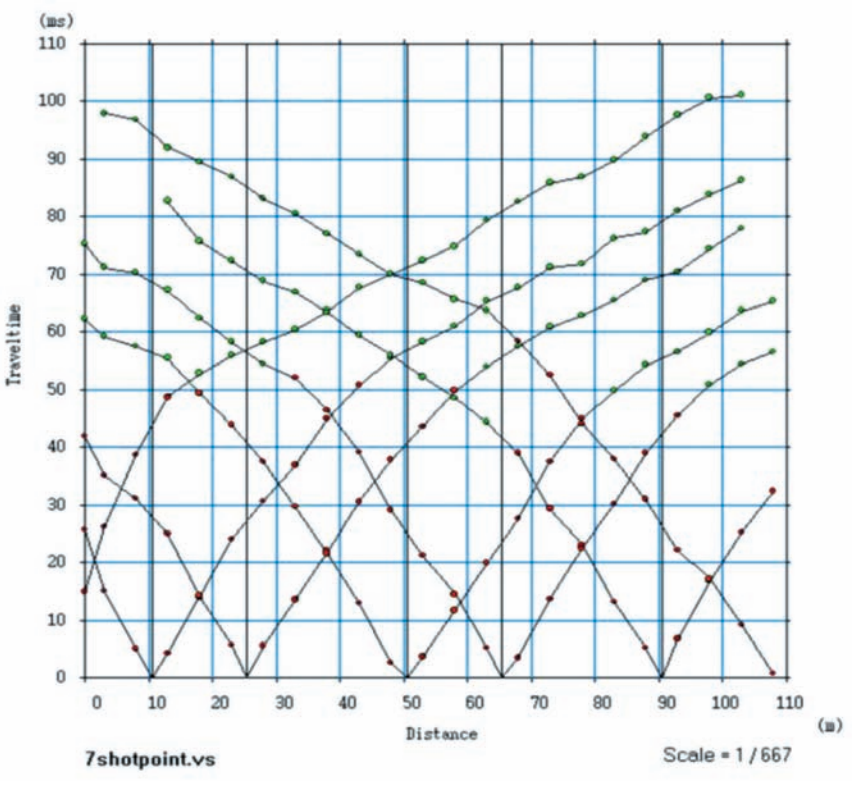

Fig. 7. Time-Distance plot of refraction field dataset.

A sledge hammer (12 kg) was used to generate the seismic signals for seismic refraction data. In the case of seismic refraction, both forward and reverse shooting were carried out along each profile over a lateral distance of 115 m. The seismic results indicated that the area is composed of two main layers that are nearly lateral (Fig. 7).

For the joint inversion procedure, a line 55 m in length was selected (Fig. 8). Similar to the inverse strategy of the synthetic cases, V_S, V_P, and thicknesses (H) of layers were considered as variables (Table 6). After a number of runs and the consideration of different models, with respect to the observed dispersion curve, a 3-layer model was adopted. The results of the V_S profile shown in Fig. 9 indicate that there was a low velocity at a depth of about 5 m. The findings introduced three layers with characteristics, presented in Table 7 and Figs. 9 and 10, that have a good correlation with detailed geological and geotechnical studies that show the upper layer is made up of soil consisting of alluvium and sandy clay and the second layer is made up of clay soil and tuff. In addition, there is a water table at a depth of about 5 m (Golpasand et al., 2013). Moreover, the results show the V_P profile in detail, and a thin layer with

a velocity of about 650 m/s was detected (Fig. 10). The objective function values over the PSO joint inversion are depicted in Fig. 11. Actually, the minimum value in Fig. 11 is the best solution for the adopted model. Furthermore, the PSO joint inversion was compared with the PSO single inversion of the ReMi data and NSGA-II approach.

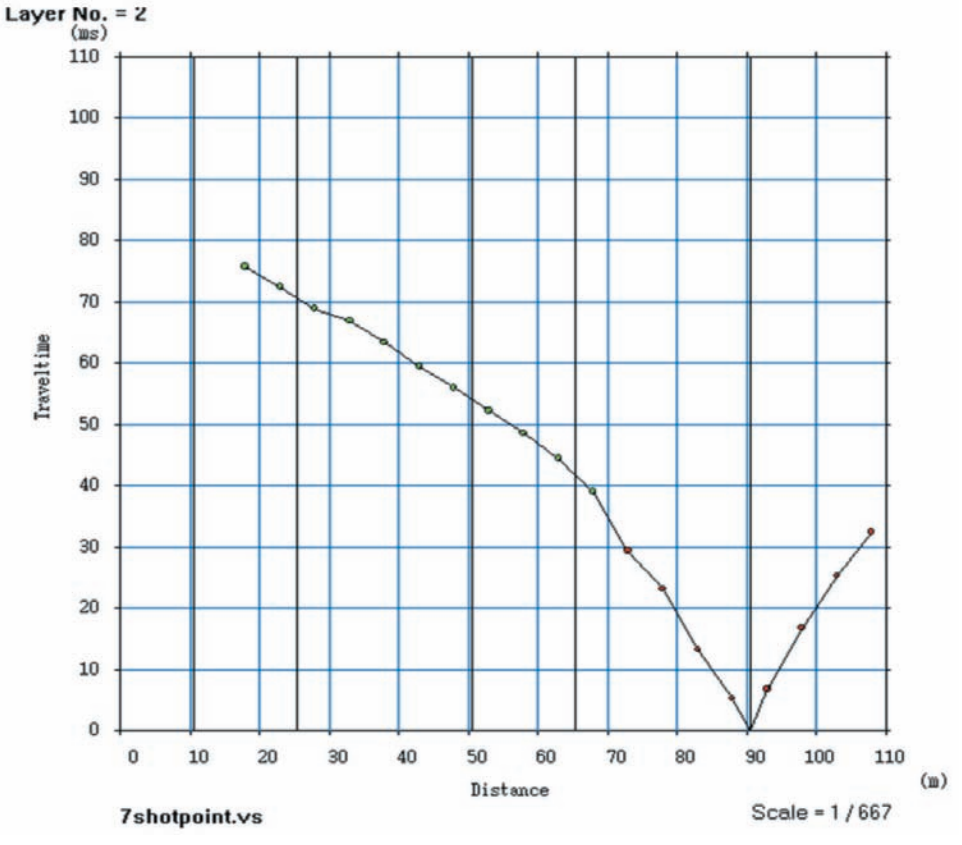

Fig. 8. Traveltime selected for PSO Joint inversion algorithm.

Table 6. Search space for PSO joint inversion of field dataset.

layer number	search space		
	thickness(m)	P-wave velocity(m/s)	S-wave velocity(m/s)
1	2-7	400- 700	150- 450
2	1-5	450- 900	200- 550
3	-	800-1600	350-750

Table 7. Mean model obtained from the field dataset.

parameters	PSO Joint Inv.	NSGA-II	PSO
H1(m)	5.5	5.53	2.6
H2(m)	2.8	1.98	4
V_P1(m/s)	507	523	680
V_P2(m/s)	657	509	473
V_P3(m/s)	1455	1114	1350
V_S1(m/s)	316	385	412
V_S2(m/s)	280	373	332
V_S3(m/s)	512	405	517

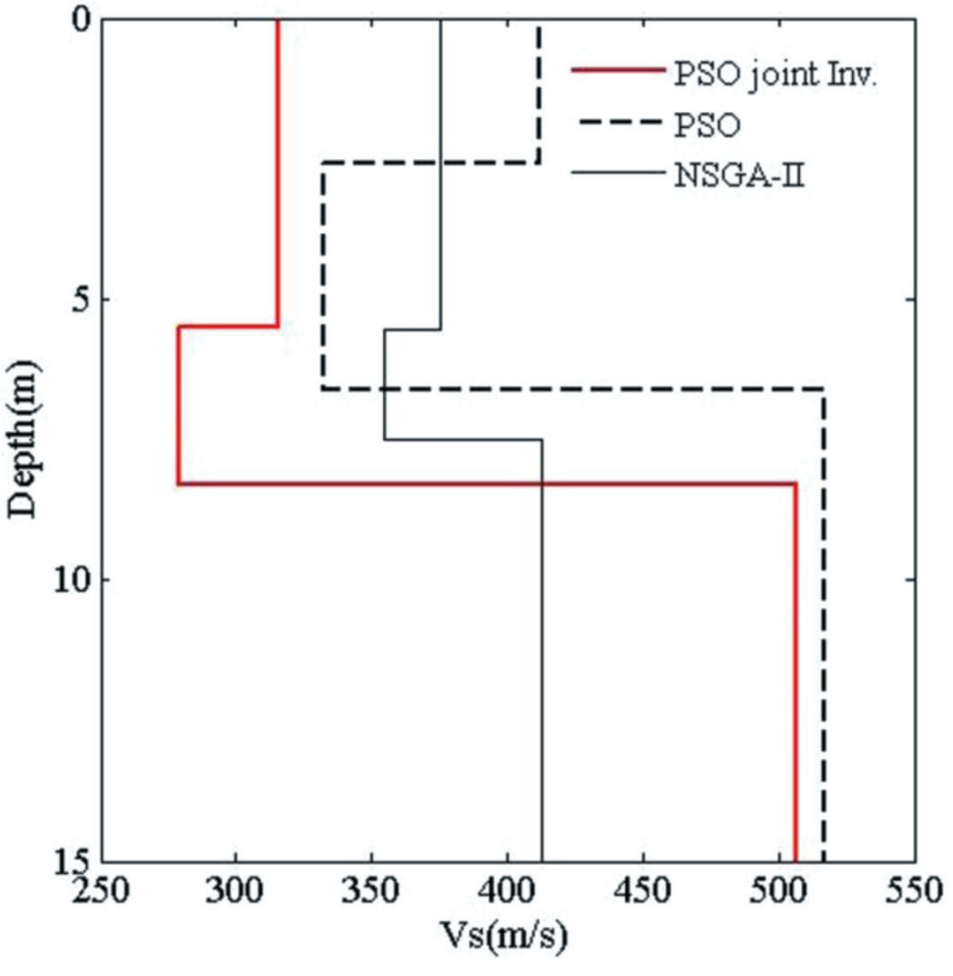

Fig. 9. Obtained S-wave structure from experimental dataset using PSO joint inversion of ReMi and seismic refraction data (PSO joint Inv.), PSO inversion of ReMi data (PSO) and NSGA-II algorithm in joint inversion of ReMi and seismic refraction data (NSGA-II).

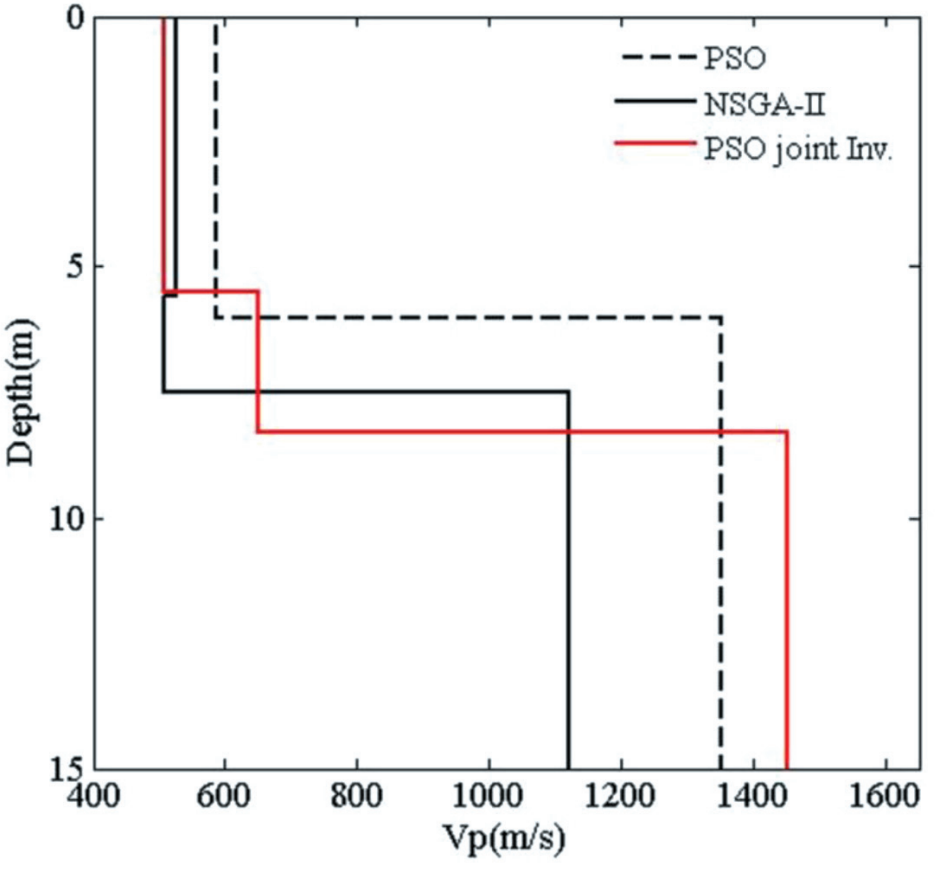

Fig. 10. Obtained V_P structure from experimental dataset using: PSO joint inversion of ReMi and seismic refraction data (PSO joint Inv.), PSO single inversion of seismic refraction data (PSO) and NSGA-II algorithm in joint inversion of ReMi and seismic refraction data (NSGA-II).

CONCLUSION

Surface wave studies and the seismic refraction method are two main seismic approaches in engineering geology and geotechnical studies. Surface wave dispersion analysis is a suitable tool for near-surface seismic characterization, but the main problem is related to the non-uniqueness of the nature of the dispersion curve inversion. To dominate this problem, a careful strategy in the inversion of a dispersion curve is needed. On the other hand, seismic refraction studies also suffer from the hidden layer and the non-uniqueness of the solution.

In order to overcome these problems, achieve a reliable interpretation, and remove any uncertainty in the results, the current study proposed a PSO joint inversion scheme. The PSO algorithm is a global optimization method

belonging to the group of metaheuristic searching algorithms. In the proposed method, refraction microtremor (as a passive seismic method) and seismic refraction data (as an active seismic method) are simultaneously inverted. The proposed method was investigated with two synthetic datasets and a real dataset. The PSO joint inversion algorithm was compared with the PSO single inversion and NSGA-II algorithms. Findings indicated that PSO joint inversion is more accurate in estimating V_S and thickness of layers than the PSO single inversion algorithm. Moreover, PSO joint inversion is more accurate, easier, and faster than NSGA-II. For a more in-depth probe, PSO joint inversion investigations with actual datasets were performed in part of the city of Tabriz in northwestern Iran. The results showed that the study area is composed of two main layers; the first layer is soil consisting of alluvium and sandy clay, the intermediate layer is a mix of clay and sand with moisture, and the last layer is made up of clay soil and tuff. Therefore, in processing the geophysical data that suffers from non-uniqueness, especially when dealing with field datasets (necessarily including a variable amount of noise), final results by joint inversion appear to be quite robust. The proposed PSO joint inversion algorithm is a high performance approach in the joint inversion of seismic data.

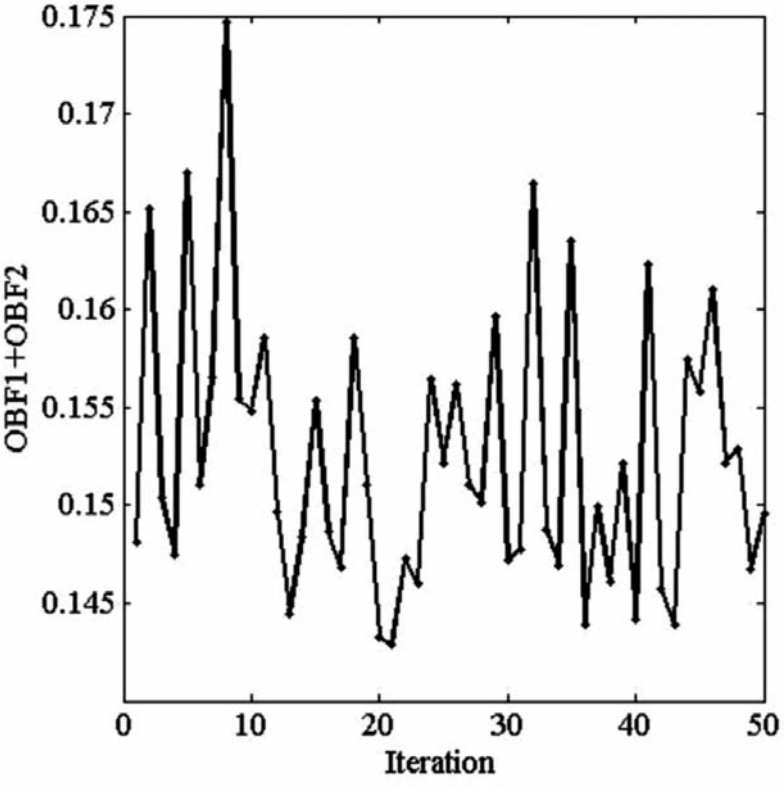

Fig. 11. Objective function (OBF) over the PSO joint inversion in experimental dataset.

ACKNOWLEDGEMENTS

We thank the Tabriz Metropolis Council for providing the experimental real data of this study. We would also like to acknowledge SeisImager Software and Service for processing our real data.

REFERENCES

Carlisle, A. and Dozier, G., 2001. An off-the-shelf PSO. Proc. of the 2001 Workshop On particle Swarm Optimization, Indianapolis: 1-6.

Cha, Y.H., Kang, J.S. and Jo. C.H, 2006. Application of linear-array microtremor surveys for rock mass classification in urban tunnel design. Explor. Geophys., 37: 108-113.

Clerc, M., 1999. The swarm and the queen: towards a deterministic and adaptive particle swarm optimization. In: Angeline, P.J., Michalewicz, Z., Schoenauer, M., Yao, X. and Zalzala, A. (Eds.), Proc. of the Congress of Evolutionary Computation. IEEE Press: 1951-1957.

Clerc, M.A. and Kennedy, J., 2002. The particle swarm-explosion, stability, and convergence in a multidimensional complex space. IEEE Transact. Evolution. Computat., 6: 58-73.

Coccia, S., Del Gaudio, V., Venisti, N. and Wasowski, N., 2010. Application of Refraction Microtremor (ReMi) technique for determination of 1-D shear wave velocity in a landslide area. J. Appl. Geophys., 71: 71-89.

Coello, C.A., Pulido, G.T. and Lechuga, M.A., 2004. Handling multiple objectives with particle swarm optimization. IEEE Transact. Evolution. Computat., 8(3): 23-38.

Dal Moro, G., 2008. V_S and V_P vertical profiling via joint inversion of Rayleigh waves and refraction traveltimes by means of bi-objective evolutionary algorithm. J. Appl. Geophys., 66: 15-24.

Deb, K., Agrawal, S., Pratab, A. and Meyarivan, T., 2000. A fast elitist nondominated sorting genetic algorithm for multi-objective optimization: NSGA-II. In: Proc. Parallel Problem Solving From Nature VI Conf.: 849-858.

Evers, G.I., 2009. An Automatic Regrouping Mechanism to Deal with Stagnation in Particle Swarm Optimization. M.Sc. thesis, Univ. of Texas-Pan American.

Fernández Martínez, J.L., García Gonzalo, E., Fernández Álvarez, J.P., Kuzma, H.A and Menéndez Pérez, C.O., 2010a. PSO: a powerful algorithm to solve geophysical inverse problems: application to a 1D-DC resistivity case. J. Appl. Geophys., 71: 13-25.

Fernández Martínez, J.L., García Gonzalo, E., Fernández Muñiz, Z., Mariethoz, G. and Mukerji. T., 2010b. Posterior sampling using particle swarm optimizers and model reduction techniques. Internat. J. Appl. Evolution. Computat., 1(3): 27-48.

Foti, S., Sambuelli, L., Socco, V.L. and Strobbia, C., 2003. Experiments of joint acquisition of seismic refraction and surface wave data. Near Surf. Geophys., 3: 119-129.

Garcia, Ch., Kang, F.J. and Tae-Seob, K., 2014. Lateral heterogeneities and microtremors: Limitations of HVSR and SPAC based studies for site response. Engineer. Geol., doi:10.1016/j.

Gardner, G.F., Gardner, L.W. and Gregory, A.R., 1974. Formation velocity and density the diagnostic basic for stratigraphic trap. Geophysics, 39: 770-780.

Golpasand, M.B., Nikudel, M.R. and Uromeihy, A., 2013. Predicting the occurrence of mixed face conditions in tunnel route of Line 2 Tabriz metro, Tabriz, Iran. In: Wu, F. and Qi, S., (Eds.), Global View of Engineering Geology and the Environment. Taylor & Francis Group, London.

Hering, A., Misiek, R., Gyulai, A., Ormos, T., Dobroka, M. and Dresen, L., 1995. A joint inversion algorithm to process geoelectric and sutface wave seismic data, Part 1: basic ideas. Geophys. Prosp., 43: 135-156.

Herrmann, R.B., 1987. Computer Programs in Seismology, User's Manual II. St. Louis University, St. Louis, MS.

Kearey, P., Brooks, M. and Hill, I., 2002. An Introduction to Geophysical Exploration. Blackwell Publications, Oxford.

Kennedy, J. and Eberhart, R.C., 1995. Particle swarm optimization. Proc. IEEE Internat. Conf. Neural Netw., Perth, Piscataway, Australia: 1942-1948.

Louie, J.N., 2001. Faster, better: shear wave velocity to 100 meters depth from refraction microtremor arrays. Bull. Seismol. Soc. Am., 91: 347-364.

Mahajan, A.K., Mundepi, A.K., Chauhan, N., Jasrotia, A.S., Rai, N. and Gachhayat, T.K., 2012. Active seismic and passive microtremor HVSR for assessing site effects in Jammu city, NW Himalaya, India, A case study. J. Appl. Geophys., 77: 51-62.

Panzera, F. and Lombardo, G., 2013. Seismic property characterization of lithotypes cropping out in the Siracusa urban area, Italy. Engin. Geol., 153: 12-24.

Pekşen, E., Yas, T.A., Kayman, Y. and İzkan, C., 2011. Application of particle swarm optimization on self-potential data. J. Appl. Geophys., 75: 305-318.

Poormirzaee, R. and Hamidzadeh, R.M., 2014. Determination of S-wave structure via refraction microtremor technique in urban area: a case study. J. Tethys, 2: 347-356.

Poormirzaee, R., Hamidzadeh, R.M. and Zarean, A., 2014a. Inversion seismic refraction data using particle swarm optimization: a case study of Tabriz, Iran. Arab. J. Geosci., in press. DOI:10.1007/s12517-014-1662-x.

Poormirzaee, R., Hamidzadeh, R.M. and Zarean, A., 2014b. PSO: a powerful and fast intelligence optimization method in processing of passive geophysical data. Proc. Internat. Conf. Swarm Intellig. Based Optimiz., Mulhouse, France: 12-19.

Rucker, M.L., 2003. Applying the refraction microtremor (ReMi) shear wave technique to geotechnical characterization. Proc. 3rd Internat. Conf. Applic. Geophys. Methodol., 8-12.

Schutte, J.F. and Groenwold, A.A., 2005. A study of global optimization using particle swarms. J. Global Optimiz., 31: 93-108.

Scott, J.B., Clark, M., Rennie, T., Pancha, A., Park, H. and Louie, J.N., 2004. A shallow shear-wave velocity transect across the Reno, Nevada, area basin. Bull. Seismol. Soc. Am., 94: 2222-2228.

SeisImager/SW Manual, 2009. Windows Software for Analysis of Surface Waves. Version 3.0. http://www.geometrics.com.

Shi, Y. and Eberhart, R.C., 1998. A modified particle swarm optimizer. Proc. IEEE Internat. Conf. Evolution. Computat., Piscataway, NJ: 69-73.

Srinivas, N. and Deb, K., 1994. Multiobjective optimization using nondominated sorting in genetic algorithms. Evol. Comput., 2: 221-248.

Stephenson, W.J., Louie, J.N., Pullammanappallil, S., Williams, R.A. and Odum, J.K., 2005. Blind shear-wave velocity comparison of ReMi and MASW results with boreholes to 200 m in Santa Clara Valley. Implications for earthquake ground-motion assessment. Bull. Seismol. Soc. Am., 95: 2506-2516.

Trelea, I.C., 2003. The particle swarm optimization algorithm: Convergence analysis and parameter selection. Informat. Process. Lett., 85: 317-325.

Xia, J., Miller, R.D. and Park, C.B., 1999. Estimation of near-surface shear-wave velocity by inversion of Rayleigh waves. Geophysics, 64: 691-700.

Yang, X.S., 2010. Engineering Optimization, Introduction with Metaheuristic Applications. John Wiley & Sons, New York: 19-22.

Zarean, A., Mirzaei, N. and Mirzaei, M., 2015. Applying MPSO for building shear wave velocity models from microtremor Rayleigh-wave dispersion curves. J. Seismic Explor., 24: 51-82.